Dynamic origin of stripe domains

G. Leaf,* H. Kaper,* M. Yan,* V. Novosad@, P. Vavassori#, R. E. Camley^ and M. Grimsditch@

Mathematics and Computer Science Division, Argonne National Laboratory, Argonne, IL 60439

INFM-CNR S3 and Dipartamento di Fisica, Universita di Ferrara, Via Saragat 1, I-44100 Ferrara, Italy.

@ Materials Science Division, Argonne National Laboratory, Argonne, IL 60439

^ Dept. of Physics, University of Colorado, Colorado Springs, CO 80918

Abstract

We investigate stripe domain formation in nanometer sized Co bars. The magnetic equilibrium states and the magnetic spin wave frequencies are obtained from micromagnetic-like simulations. We find that the lowest frequency standing wave mode has the same spatial structure as the stripe domains at remanence and it goes soft at the field where the stripe domains emerge. We show, therefore, that the final domain structure at remanence, which is not the configuration with lowest energy, is predicted from a high-field analysis of the frequencies of the standing spin waves.

PACS 75.75.+a, 75.40.Mg, 75.40.Gb

Stripe-domains are common to a wide variety of physical phenomena. They are known to arise from an interplay between short- and long-range forces. Landau and Lifshitz [1] were the first to propose a formalism that describes the energetics of stripe domain formation. This formalism concentrates on energy considerations and it is easy to see that the formation of stripe domains can lead to a reduction of the total energy of the system. However, it is unclear how a system evolves into a particular stripe domain pattern.

In spite of its long history, stripe domains are still the subject of intense scrutiny. Some recently investigated systems that exhibit stripe domains include: block-copolymers[2], thin ferroelectric films[3], domains expected in a 'striped quantum liquid crystal' are compared with those in an Fe film [4], and a 'topological order parameter' is found for stripe domain formation in a 'planar t-Jz Model'[5].

The case of stripe domain patterns forming in thin ferromagnetic layers with large magnetic anisotropies perpendicular to the surface has been widely investigated. Although the <u>energy</u> conditions for the formation of the observed patterns (parallel, labyrinthine, bubble-like) are understood in terms of the anisotropy, exchange and magnetostatic energies, [6, 7] the process through which the magnetization breaks up into stripes is still unclear.

Here we investigate this issue by studying the magnetic normal modes of a nanoscale cobalt bar with competing in-plane uniaxial and shape anisotropies. Although such a system is known to develop stripe domains at remanence [8], there are many general questions relating to the final configuration. (Here we deal with the particular case of a field applied along the long axis of the bar). These include:

1) Is the final configuration at remanence the lowest energy state?

2) Is the final configuration in these small structures determined by what happens at the ends of the bar?

3) Can the final configuration at H = 0 be predicted from the behavior of the system at large fields where the magnetization is saturated?

4) Is there a connection between a soft mode and the final state found at remanence?

We find that the configuration at remanence is not the lowest energy state. In systems showing hysteresis this would not be surprising. However, in cases like ours with negligible hysteresis (See the loop in the inset to Fig. 1) it is often assumed that the system follows its global minimum energy state and that the stripe domains at remanence correspond to this energy minimum. More interestingly, we find that the period of the domains at remanence is determined by the wavelength of the lowest frequency 'bulk' normal mode at external magnetic fields well above the onset of domain formation. Finally, we show that this lowest frequency bulk mode goes soft at the same field where domains emerge. Although the results that will be presented here refer to a laterally confined system, the same origin can be envisioned for stripe domains in thin films.

The equilibrium magnetic configurations were obtained using a micromagnetic code described earlier [9] with a finite damping coefficient. The extension of this code that enables the frequency and spatial structure of the magnetic normal modes to be calculated has been described in [10]. This method involves calculating the time evolution of the system with zero damping and performing a Fourier transform to obtain the frequency response. We also use OOMMF [11] for some micromagnetic calculations; this method and the code in [9] give almost identical results for the static configurations.

We consider a single crystal *hcp* Co bar, 40 nm thick and 120 nm wide, with an in-plane uniaxial anisotropy and lengths of either 792 or 936 nm. In the discretization we use cubic cells with a side length of 8 nm. Smaller cell sizes can be used for the equilibrium simulations but this produces negligible changes to the energies or magnetic configurations. However, because of the computation demands of the normal mode dynamics, for internal consistency we use 8nm cells for both sets of calculations. For the long wavelength modes investigated here 8nm cells should be perfectly adequate. Reducing the sample size so that smaller cells can be used in the simulation leads to soft modes with fewer nodes which then become less easy to distinguish from end modes and thus make the interpretation less clear. The long edges are aligned perpendicular to the c-axis to allow the shape anisotropy to compete with the magnetocrystalline anisotropy. This competition is known to lead to the formation of stripe domains at remanence when the external magnetic field is applied along the long edge of the bar [8]. The input material parameters for both calculations are the saturation magnetization Ms=1.4 x 10^5 A/m, the exchange constant A = 3 x 10^{-11} J/m and the uniaxial anisotropy constant K_u= 5.2 x 10^5 J/m^3; all of them are typical values for epitaxial cobalt films.

As discussed in the introduction we address the question of what determines the ground state configuration of the magnetic bar and whether this configuration is somehow related to a soft-mode behavior. Before we begin the discussion of the dynamics, we note that, even in the same particle, different field histories can lead to dramatically different stripe domains. Below we describe three different processes and the key outcomes. (i) A large field is applied along the long axis of the 792 nm bar. As the field is reduced the bar breaks up into 11 stripe domains. (ii) A large field is applied along the short axis of the 792 nm bar, along the uniaxial direction. As this field is reduced and then made negative, the bar breaks up into 5 domains. If the magnetic field is then reduced to zero, the 5 domain state remains stable. (iii) A large field is applied at an angle to the short axis of the 792 nm bar. As this field is reduced and then made negative, the bar breaks up into 3 domains. Again, this state is stable at zero applied field. All of these domain patterns are stable and hence in local energy minima, none of them correspond to the absolute energy minimum with 6 domains (i.e 5 domain walls) (see Fig. 1).

The belief that energy minimization is the key ingredient of any model that explains stripe domain formation must therefore be questioned. From micromagnetics, it is possible to find the ground state energy of a bar with any number of domains simply by choosing different initial conditions or field history. In Fig. 1 we plot the total energy at zero applied field for the 792 nm bar as a function of number of (nearly evenly spaced) domains. From this figure one might conclude that the 6 domain state ought to occur at H = 0, rather than any of the domain states described above.

We now turn to a detailed examination of the domain formation process for the case where a large magnetic field is applied along the long axis of the bar and then reduced. The spin configurations at various external field values are shown in Fig. 2 (a) – (d). It is clear from these diagrams that the magnetization evolution is a complex process initiated at the particle ends and that the initial deviations from saturation bear little resemblance to the domain structure at remanence. Based on this figure, it is tempting to attribute the formation of stripes to “end effects’’. However simulations on bars that differ only in length show that the typical size of the domains is the same in all bars – indicating that the final state is a bulk-like phenomenon.

The frequencies of the normal modes at each field give us additional insight into the nature of the phase transition. These modes can be roughly classified as localized modes, which include end modes, corner modes, and edge modes, and bulk modes, which resemble standing wave like solutions and have long-axis wavevectors $q \approx n\pi/L$ (where n is an integer and L is the length of the sample). Here we deal in detail with the bulk modes; the influence of the localized modes will be discussed in a later paper.

In Fig. 3 we have plotted the frequency of the standing wave modes as a function of the wavevector, q, for three cases; the long bar at H = 7 kOe, the long bar at H = 6 kOe and, the short bar for H = 6 kOe. The spin excitations have wavelengths which vary slightly across the length of the bar, so we have chosen to calculate q by using the wavelength found in the central portion of the bar. The important point is that the lowest frequency mode is always the one with $q = 0.043\ \text{nm}^{-1}$ independent of length of the bar or the magnitude of the applied field. This wavevector corresponds to a wavelength of about 146 nm. If we consider the 11 domain structure in the short bar we find that the average domain size is 72 nm. (The domain sizes are not perfectly uniform either.) Since one wavelength should correspond to two domains, one wavelength would be 144 nm, in excellent agreement with the result found in the dynamical calculation. One finds exactly the same number, 144 nm, for the average domain size in the longer bar as well. These facts indicate that this domain structure is caused by a "bulk" mode and not a configuration induced by end effects.

A "snapshot" of the out of plane component of the precessing magnetization for the lowest frequency mode at 12 kOe is shown in both contour and 3D and formats in Figs 2e and f. Since the applied field is 12 kOe there are no domains in the bar and the magnetization is essentially saturated and not very different from that shown in Fig. 2a.

Although the frequency of this mode decreases as the field is reduced, its shape (Figs 2e and 2f) remains essentially unchanged. It is clear that the wavelength of this mode closely matches the typical domain size observed in the 13 domain state found in the micromagnetic simulations and shown in Fig. 2d. For the short particle the mode with lowest frequency has 11 nodes and leads to a structure with 11 domains.

In our view the remanent structure in Fig. 2d and the soft mode are related as follows: In the correlated spin motion of the mode shown in Figs. 2e and f, at given instants of time, the spins in the blue and red regions (Fig. 2e) will have opposite components along the width direction. When the restoring force vanishes, i.e the frequency goes to zero, this wave-like pattern freezes and provides the nucleus on which the stripe domains grow.

Since the minimum frequency in Fig. 3 is quite flat, one can argue that the soft mode in a real system could easily be any of the lowest modes and that that could lead to a different number of domains at remanence. Although true for a real sample with imperfections or at a finite temperature, in our micromagnetic simulations the path is fully deterministic (excluding numerical round-off errors) and we find that, for a given particle and field history, the sample always has the same number of domains at remanance. If we could perform micromagnetic simulations that include the effects of temperature or structural variations, we expect that, statistically, we might obtain remanent states with 9 through 15 domains. This however would not change our claim that stripe domains have a dynamic origin in each case.

In Fig. 4 we have plotted the frequency of the lowest frequency bulk mode (the one shown in fig. 2) as a function of field. For comparison, we also show the frequency of the uniform mode, the one which would be observed by ferromagnetic resonance. Although they are not shown, at high fields there are many end modes that lie below the bulk modes, however, when the external field is reduced to around 5kOe, the soft bulk mode has the lowest frequency of all the modes in the bar and approaches zero frequency just below H = 5 kOe. Thus in this geometry, the final state configuration is directly connected with a particular bulk mode which is driven to zero frequency.

Fig. 4 also shows the evolution of an order parameter as a function of applied field. The squares in Fig. 4 are the maximum value of $|M_z|$ in the cells in the central portion of the bar where z is the easy axis for the uniaxial anisotropy; as such it provides a convenient order parameter for the transition to a stripe domain pattern. Noting that the order parameter and the frequency of the lowest bulk mode extrapolate to zero at the same field (within the simulation uncertainty), and also that the contour plot in Fig 2e (at 12 kOe) has identical symmetry as the stripe domains at remanence in Fig. 2d, (0 kOe) we claim that the origin of stripe domains in this system is a soft magnon mode, and not the minimization of energy.

We note that the method of calculating the eigenmodes by following the time-evolution of the structure is only one approach to understanding the behavior of this system. We have also used a dynamical matrix approach to calculate all the eigenmodes of the system at any applied field. With this method we again find that at a field slightly above the phase transition all the modes have a positive frequency, indicating a stable structure. However as the field is reduced one mode, the same bulk mode discussed above, is driven to zero frequency and the system undergoes a phase transition. We have also investigated the relationship between other instabilities in the magnetic structure (such as the appearance of C- and S-states and the 3 and 5 domain states mentioned earlier) and soft magnetic modes. In all cases we find that instabilities occur in the vicinity of soft mode behavior. Except for the example presented here all other instabilities we observed involved edge- or end-like modes.

Since these types of modes have not yet been described in the literature and since they also depend on particle shape, their behavior, although fascinating, does not have the generality of soft bulk modes. Due to space limitations these studies will be presented elsewhere.

In summary, we have studied the origin of stripe domains in anisotropic ferromagnetic particles using micromagnetic simulations to obtain the equilibrium states and calculations of the particle normal modes to probe magnetization dynamics. We find that a standing wave mode with a particular wavelength consistently has the lowest frequency of all the standing spin modes, independent of applied magnetic field or length of the bar. The wavelength of this mode coincides with that of the stripe domain magnetization profile at remanence. Furthermore, this particular mode is driven to zero frequency at a field near 5 kOe, the field at which the stripe domain order parameter assumes a non-zero value. From this we infer that the origin of the domain pattern at remanence is contained in a soft magnetic mode, and the final domain pattern is predictable from the dynamic behavior at high magnetic fields.

VN and MG were supported by the US DOE-BES under contract N° W-31-109-ENG-38. GL, HK and MY were supported by the Mathematical, Information and Computational Sciences Division of the office of Advanced Scientific Computing Research of the US DOE under contract W-31-109-Eng-38. REC acknowledges support from the Argonne Theory Institute. PV acknowledges support from the projects FIRB RBNE017XSW and PRIN2004027288 of MIUR.

References

1 L. Landau and E. Lifshitz. Phys. Zs. Sow. **8**, 153 (1935) and *Electrodynamics of Continuous Media*, Pergamon, Oxford (1960)

2 C. Harrison, D. Adamson, Z. Chen, J. Sebstian, S. Sethuraman, D. Huse, R. Register and P. Chaikin. Science **290**, 1558 (2000)

3 S. Streiffer, J. Eastman, D. Fong, C. Thompson, A. Mumkholm, M. Ramana Murti, O. Auciello, G. Bai and G. Stephenson. Phys. Rev. Lett **89**, 067601 (2002)

4 O. Portmann, A. Vaterlaus and D. Pescia. Nature **422**, 701 (2003)

5 J. Smakov, D. Batista and G. Ortiz. Phys. Rev. Lett. **93**, 067201 (2004)

6 R. Allenspach and R. Bischof PRL 69, 3385 (1992); A. B. Kashuba and V. L. Pokrovsky PRB 48, 10335 (1993); Y. Yafet and E. M. Gyorgy PRB 38, 9145 (1988); R. Allenspach, M. Stampanoni, and A. Bischof PRL 65, 3344 (1990); M. Hehn, S. Padovani, K. Ounadjela, and J. P. Brucher PRB 54, 3428 (1996); M. –T. Lin, J. Shen, W. Kuch, H. Jenniches, M. Klaua, C. M. Schneider, and J. Kirschner PRB 55, 5886 (1998).

7 A. Hubert and R. Schäfer, *Magnetic Domains* (Springer, Berlin 1998) and references quoted therein.

8 T. Kohda, Y. Otani, V. Novosad, K. Fukamichi, S. Yuasa, M. Nyvlt, T. Katayama, IEEE Trans Magn **35**, 3472 (1999).

9 J. S. Jiang, H. Kaper and G. Leaf. Discrete Contin. Dyn. Syst. Ser B. **1**, 219 (2001).

10 M. Grimsditch, G. Leaf, H. Kaper, D. Karpeev and R. Camley. Phys. Rev. B. **69**, 174428 (2004)

11 M. J. Donahue and D. G. Porter, *OOMMF User's Guide, Version 1.2 alpha 3* (National Institute of Standards and Technology, Gaithesburg, MD, 2002)

Figure Captions

1) Energy as a function of number of domains for the 792 nm bar in zero field. The insert is the hysteresis loop for a field along the long axis.

2) a-d Static magnetization configurations for a 936 nm Co bar at different magnetic fields applied along the long axis of the bar. The red and blue colors are guides to the eye indicating up and down magnetization respectively. Panels (e) and (f) give a snapshot of the out-of-plane component of the precessing magnetization of the lowest frequency standing wave at 12 kOe. The contour representation of the wave (e) and is remarkably similar to the final domain pattern found at H = 0 (c).

3) Frequency as a function of wavevector for standing-wave modes in both the long (936 nm squares and circles) and short (792 nm triangles) bars and for two different magnetic fields. Note that in all cases the minimum frequency occurs near q = 0.043 nm^{-1} which corresponds to a wavelength of 144 nm and hence to 13 and 11 domains in the two particles respectively.

4) Frequency as a function of applied magnetic field for the lowest frequency bulk mode and the uniform resonance mode (right axis). The left hand side shows the evolution of the "order parameter" $|M_z|$ in the central region of the bar.

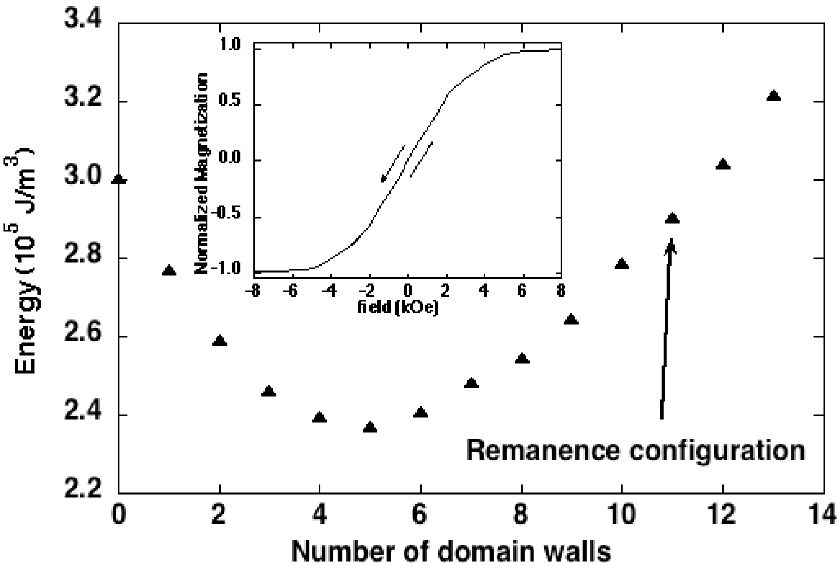

Figure 1: Energy as a function of number of domains for the 792 nm bar in zero field. The insert is the hysteresis loop for a field along the long axis.

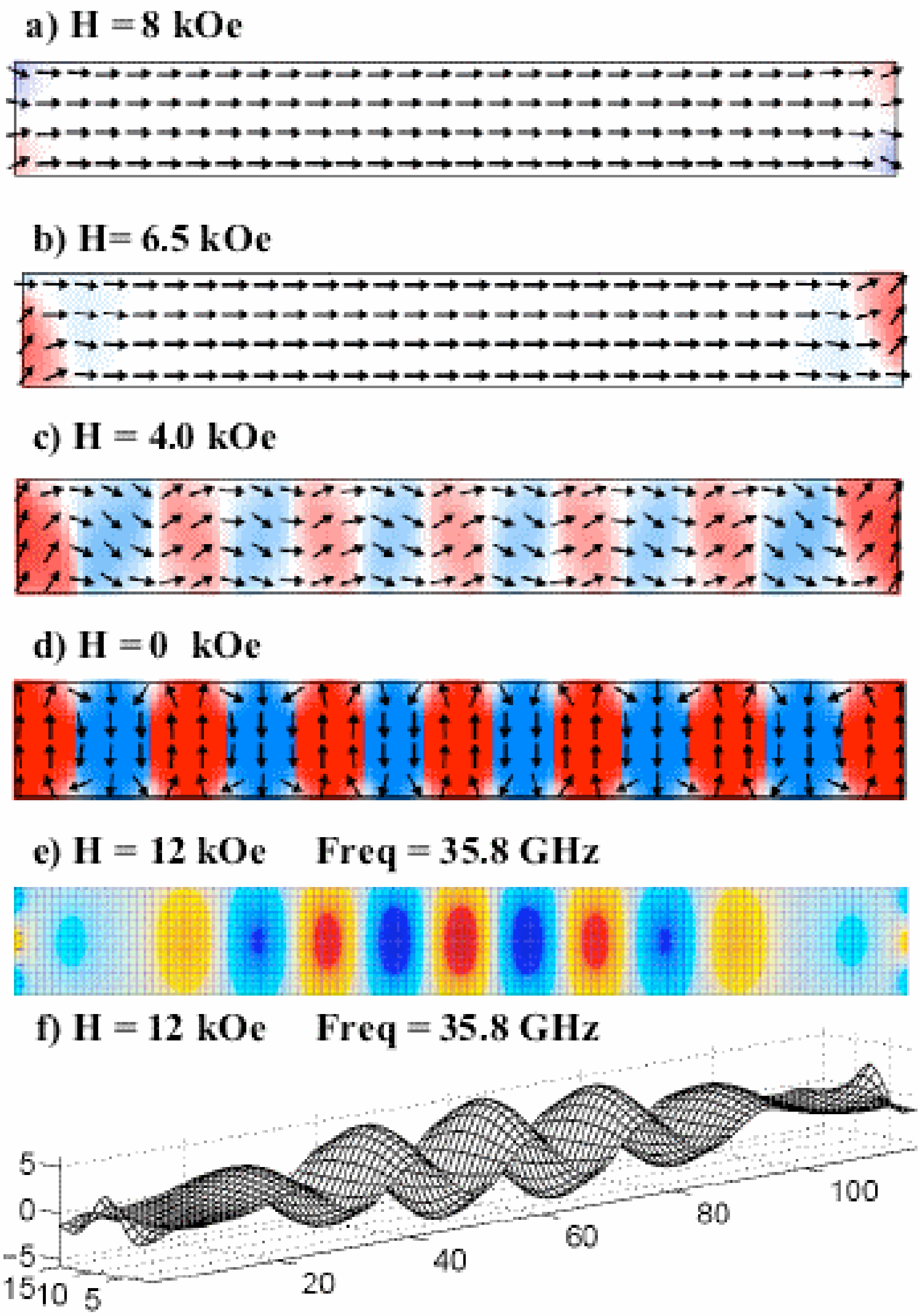

Fig. 2 a-d Static magnetization configurations for a 936 nm Co bar at different magnetic fields applied along the long axis of the bar. The red and blue colors are guides to the eye indicating up and down magnetization respectively. Panels (e) and (f) give a snapshot of the out-of-plane component of the precessing magnetization of the lowest frequency standing wave at 12 kOe. The contour representation of the wave (e) and is remarkably similar to the final domain pattern found at H = 0 (c).

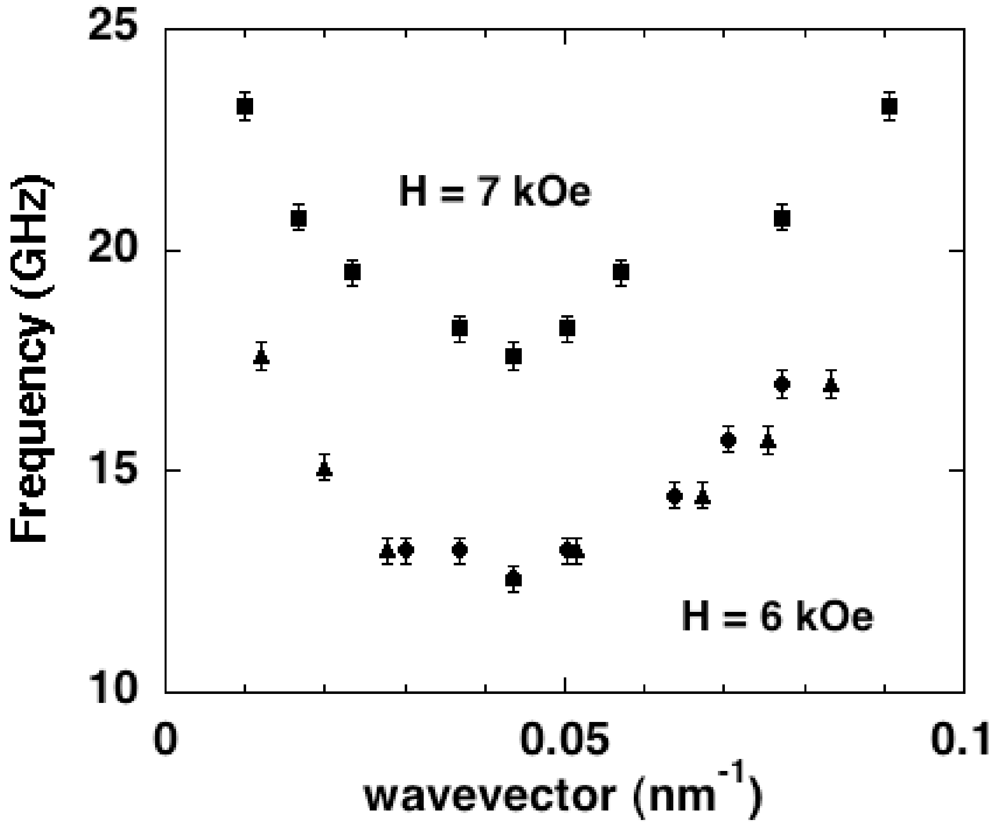

Figure 3: Frequency as a function of wavevector for standing-wave modes in both the long (936 nm squares and circles) and short (792 nm triangles) bars and for two different magnetic fields. Note that in all cases the minimum frequency occurs near q = 0.043 nm^{-1} which corresponds to a wavelength of 144 nm and hence to 13 and 11 domains in the two particles respectively.

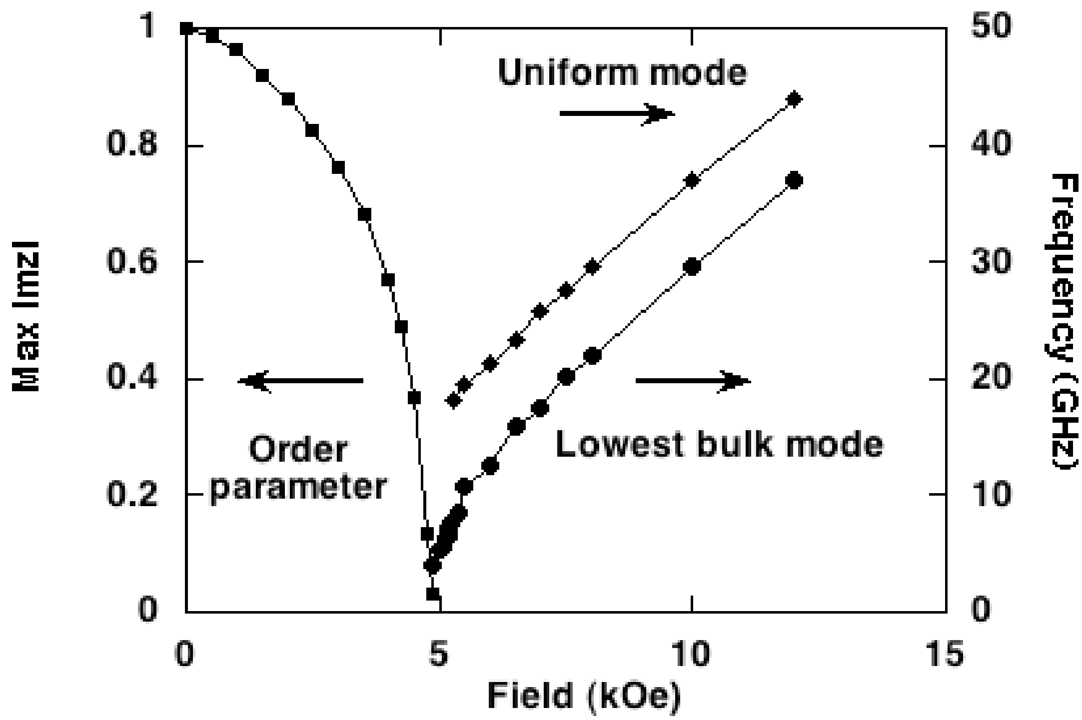

Figure 4: Frequency as a function of applied magnetic field for the lowest frequency bulk mode and the uniform resonance mode (right axis). The left hand side shows the evolution of the "order parameter" $|M_z|$ in the central region of the bar.